Synthesis and characterization of MK/Slag geopolymer composites enhanced by various ratios of nano kaolin

Hisham Mustafa Mohamed KHATER ▪ Housing and Building National Research Centre (HBNRC), Cairo ▪ Hkhater4@yahoo.com
Hamdy A. ABDEL GAWWAD ▪ Housing and Building National Research Centre (HBNRC), Cairo
Érkezett: 2017. 03. 13. ▪ Received: 03. 13. 2017. ▪ https://doi.org/10.14382/epitoanyag-jsbcm.2017.8

Abstract
Alkaline activation of slag – metakaolin (AAS) binder enhanced with nano-kaolin for preparation of eco-friendly geopolymer materials (40:60 wt. %), of geopolymer binder results in formation of C-A-S-H as well as N-A-S-H gel. Activators used are 10% NaOH solution in addition to 5% liquid sodium silicate both used from the total binder weight), while nano-kaolin was added in the ratio from 0 up to 9% from the total dry weight and replaced the used metakaolin. The properties of the produced geopolymer bricks have been studied through measurement of compressive strength, FTIR, XRD and SEM imaging. Results demonstrate enhancement in both mechanical and microstructural characteristics with nano-kaolin up to 5%, while further increase resulted in agglomeration and strength decrease, also uses of additional activators as sodium aluminate in the ratio of 5% results in strength decline as a results of zeolite increase.
Keywords: Nano-kaolin, Geopolymer, activation, eco-friendly.

Hisham Mustafa Mohamed KHATER
Ph.D. in Physical Chemistry, 2009. Associated Professor in Cement chemistry and Raw Building Materials Technology and Processing since 2015. Researcher in Raw Building Materials Technology and Processing Research Institute, Housing and Building National Research Center (HBRC). Supervisor of XRF laboratory for the chemical analysis of all type of raw building materials, accredited from International American Service IAS 17025 since 2005. Research interest: X-ray fluorescence spectroscopy, X-ray diffraction, Fourier Tranformer-IR spectroscopy, differential thermal analysis, chemical analysis of cements, recycling of waste materials, assessment of clay minerals, low cost and environmentally green building materials, nanotechnology in building materials. Author of more than 20 papers.

Hamdy A. ABDEL GAWWAD
Researcher in Raw Building Materials Technology and Processing Research Institute, Housing and Building National Research Center (HBRC). Research interest: alkali activated geopolymers, carbon nano-tubes, supplementary cementing materials

1. Introduction

Alkali activated cements refer to any system uses an alkali activator to initiate a reaction or a series of reactions which will produce a material with cementitious property. Alkali activated cement, alkali activated slag and fly ash, and geopolymers are all considered to be alkali activated cementitious systems, however, it is expected that the structures of these materials are vastly different and result from different chemical mechanistic paths. It is commonly acknowledged that calcium silicate hydrate (CSH) is the major binding phase in Portland cement [1, 2] and alkali activated slags [3]. However, the binding property of geopolymers is generally assumed to be as the result of the formation of a three-dimensional amorphous aluminosilicate network [4–6]. Davidovits stated that geopolymers formed by polymerization of individual aluminate and silicate species, dissolved from their original sources at high pH in the presence of alkali metals [6-7]. The resultant products are reported to have the general formula $Mn–[[–Si–O_2]z–Al–O]_n$- wH_2O where M is the alkali element, –indicates the presence of a bond, z is 1, 2 or 3 and n is the degree of polymerization. Theoretically, any cations in the medium can be used in balancing the three dimensional network, however sodium (Na^+) and potassium (K^+) ions are the most common univalent cations [7, 8].

Major difference between geopolymers and Portland cement in terms of chemical composition is calcium, where calcium is not essential in any part of a basic geopolymeric structure, but can form CSH which form nucleation sites for geopolymer accumulation. On the other hand, CSH which is the most important binder in cement formed as a results of hydration of tri-calcium silicate and di-calcium silicate.

Recently, many studies conducted on various metakaolin (MK)/ lime (calcium hydroxide) and MK-blended cement systems [9, 10]. Cabrera and coworkers [10, 12, 13] found that activation of metakaolin in the presence of calcium hydroxide caused rapid formation of CSH, C_2ASH_8 (stratlingite) and C_4AH_{13} (tetracalcium aluminate hydrate). Alonso and Palomo [9, 11] found alkaline activation of metakaolin in the presence of calcium hydroxide in a highly alkaline environment, led to formation of an amorphous sodium aluminosilicate, with the same characteristics as a geopolymeric gel. This geopolymeric gel formed was found to be similar to that obtained when metakaolin was activated in the absence of calcium hydroxide, in addition to a secondary product which is CSH gel. There are many factors affecting the nature of the end alkaline product [9, 10] such as: elemental composition, mineralogy, physical properties (e.g. surface properties, particle size distribution) of both aluminosilicate and calcium sources, alkalinity, nature of soluble alkaline metal present, as well as curing conditions and use of any pre-treatment. The chemical reactions that take place in the MK/GGBFS system are expected to be more complex than in the MK/lime system, as GGBFS consists of a mixture of glassy phases reacting at different rates depending on the ratio of water cooled slag to metakaolin and molar ratio of Na_2O/SiO_2 molar ratio.

Uses of nano-particles in cement and concrete can lead to improvements in the nanostructure of building materials [14]. Nano-materials show unique physical and chemical properties that can lead to the development of more effective materials than ones which are currently available [15]. The extremely fine size of nano-particles yields favorable characteristics. Ginebara et al. [16] reported that the particle size can greatly affect the hydration kinetics of cement. Ultra small magnetic ferrite

Oxide content (%)	SiO_2	Al_2O_3	Fe_2O_3	CaO	MgO	SO_3	K_2O	Na_2O	TiO_2	MnO	P_2O_5	Cl^-	L.O.I.	BaO	SrO	Total
Water-cooled slag (GGBFS)	36.67	10.31	0.50	38.82	1.70	2.17	1.03	0.48	0.57	4.04	0.04	0.050	0.12	3.28	0.18	99.96
Kaolin	56.33	27.61	1.32	0.18	0.06	0.06	0.04	0.08	3.73	-	0.13	0.05	10.17	-	-	99.97
MK (fired kaolin at 800°C for 2 hrs)	57.50	35.10	1.59	0.64	0.17	0.25	0.15	0.12	2.85	0.00	0.13	0.06	1.14	-	-	99.70
Nano-kaolin	57.53	38.63	0.35	0.11	0.30	0.56	0.03	0.01	1.02	0.01	0.41	-	0.93	-	-	99.88

Table 1. Chemical composition of starting materials (Mass, %)
1. táblázat Alapanyagok kémiai összetétele (m%)

nano particles (diameter smaller than 15 nm) when dispersed in liquid carrier possess both fluid and magnetic properties, and may lead to numerous industrial applications [17]. Several studies were performed concerning with applications of nanotechnology and nano materials in Construction [18-20], whereas nano-kaolin considered to be high reactive and low price nano-material which can be used as alternative to the high price nano-materials. Where, nano-silica and nano-alumina are mainly constituents present in nano-metakaolin (NMK) chemical structure. Various improvements obtained when NMK used as cementitious materials due to its high pozzlolanic activity [21].

Several author used NMK to improve the physico-mechanical properties and durability of cement mortar. Morsy et al. [22] reported an increase in compressive strength by 18% when adding 6% NMK compared to control cement mortar. Also, a significant increase in the compressive and flexural strength was observed when different amount of NMK added to cement mortar containing fly ash [23]. The fire resistant of cement mortar with or without NMK was studied by Morsy et al. [24]; they showed that cement mortar containing 10 and 15 wt.% NMK exhibited slow decrease in compressive strength compared to control sample as the exposure temperature increased up to 800°C. On the other hand, Baueregerm and co-authors [25] found an enhancement of 50 and 60% in the 16 hr early compressive and flexural strength, respectively, by the addition of 5% NMK to Portland cement.

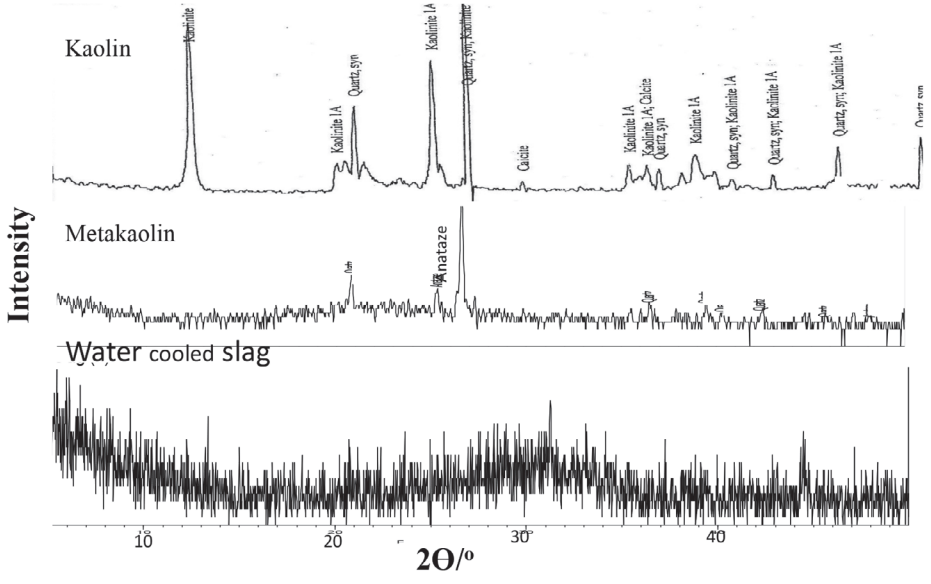

Fig. 1. X-Ray diffraction pattern of the starting raw materials
1. ábra Alapanyagok röntgendiffraktogramjai

There are few researches studied the impact of nano-kaolin on the properties of geopolymer based binder. Khater and co-authors studied the effect of NMK on the physico-mechanical properties of alkali activated slag geopolymer [26]. They found better enhancing in the mechanical properties of geopolymer by addition of 1% NMK compared with control mix up to 90 days, while higher ratio leads to matrix dilution and so negatively affect mechanical characteristics of the resulting products.

The main purpose of this work is to demonstrate the activation and enhancement effect of nano-kaolin materials on the performance of the produced geopolymer materials by alkaline activation of amorphous water cooled slag/Mk materials, where this target can be fulfilled by tracing of the hardened geopolymeric products by X-ray diffraction, FTIR and SEM are used for scanning and analysis of the composite structure of nano geopolymer. While, the compressive strength measurement was used to evaluate the mechanical performance of the geopolymer mixes.

2. Experimental procedures

2.1. Materials

Studied materials are water cooled slag sourced from Iron and Steel Factory-Helwan, Egypt, and Kaolinite material collected from El-Dehesa, South Sinai, Egypt, both chemical composition illustrated in Table 1. Sodium hydroxide (NaOH) with purity 99% in the form of pellets used as alkali activators, obtained from SHIDO Co., Egypt, while liquid sodium silicate (LSS, Na_2SiO_3. $9H_2O$) from Fisher company consists of 32% SiO_2 and 17% Na_2O with Silica modulus SiO_2/Na_2O equal 1.88 and its density is 1.46 g/cm^3, also laboratory prepared sodium aluminate with 47% Al_2O_3 and 48.10% Na_2O. Kaolinite material used for Nano-kaolin (NK) preparation brought from Middle East for Mining Investment Co., Egypt.

Composition of the starting raw materials is illustrated in *Table 1*, while mineralogical characterization of the raw materials is represented in *Fig. 1*. Water cooled slag is a rich aluminosilicate material and composed from the dominant content

of SiO_2, CaO, Al_2O_3 Fe_2O_3,and MnO as illustrated from *Table 1*, while its mineralogical composed of amorphous materials.

Whereas, the chemical composition of kaolin showed that it contains high percentage of alumina of about 56% with about 27% of silica, in addition to little amount of calcium and magnesium as presented in *Table 1*, however the mineralogical composition indicated that kaolinite composed of minor amount of quartz minerals 30% and 70% kaolin, whilst NK composed of about 95% pure kaolin and 5% quartz. This kaolinite material was thermally treated at 800°C for 2 hrs with a heating rate of 5°C /min., to form MK. This temperature was chosen on the basis of an earlier research works, where calcinations below 700°C results in a less reactive metakaolinite with more residual kaolinite, above 850°C crystallization occurs and reactivity declines [27-30].

2.2 Synthesis of NK

Kaolin nanoparticles are synthesized by firing ultra-pure kaolin at 800°C for 2 hrs with a heating rate of 5°C/min to form an amorphous nano precursors, where firing results in the formation of NK particles with the average particle size 35-53 nm, while its raw material before firing has a grain size about 100% < 10 μm as indicated from the TEM (see *Fig. 2*). *Fig. 3* illustrates XRD pattern of fired treated and untreated kaolin materials, the pattern reflects that mostly all the kaolin residues are distorted and dehydrated forming amorphous NK material.

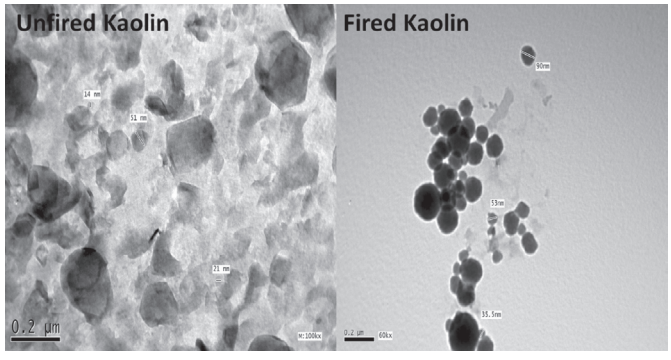

Fig. 2. Transmission electron micrograph of fired and unfired Kaolinite material provided from Middle East for mining investment
2. ábra Kiégetett és eredeti kaolin elektronmikroszkópos felvételei (forrás: Közel-Keleti bányafeltárás)

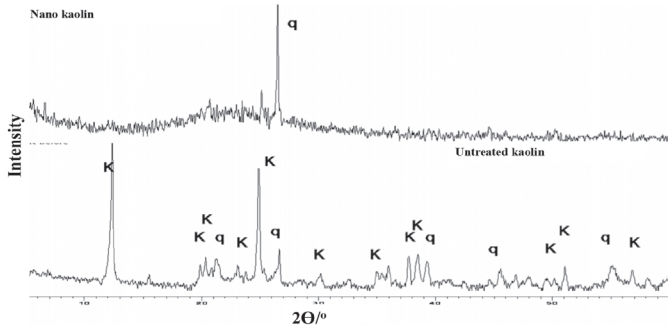

Fig. 3. X-Ray diffraction pattern of kaolin material before and after firing (provided from Middle East for mining investment) (K: kaolin, Q: quartz)
3. ábra Kiégetett és eredeti kaolin röntgendiffraktogramjai (forrás: Közel-Keleti bányafeltárás) [K: kaolin, Q: kvarc]

2.3. Geopolymerization and curing

Geopolymer made by hand-mixing raw materials of each mixture passing a sieve of 90 μm with the alkaline solution for 10 min and a further 5 min with a mixer. All investigations involved using 15 % NaOH and 5 % Na_2SiO_3 of dry mixes, while uses an additional 5% sodium aluminate as a method for comparative activation. The water-binder material ratio (w/b) was in the range of 0.22:0.24 by mass. NK was added to the binding material (Blast furnace slag and metakaolin in the ratio of 40: 60, wt.%) in small quantities 0 up to 9% from the total weight and as a replacement of metakaolin as illustrated in Table 2, mixed well with part of the total water using a magnetic stirrer, the other part of water is mixed with the activators, then added to the binding material in the mixer followed by the deflocculated NK, and finally superplasticizer (Glenium Ace) in the range of 1.50 : 2.30 %. Paste mixture were cast into 25×25×25 mm cubic-shaped moulds, vibrated for compaction and sealed with a lid to minimize any loss of evaporable water.

All mixes were left to cure undisturbed under ambient temperature for 24 hrs, followed by curing temperature at 40°C with a 100 % relative humidity. At the end of the curing regime, the specimens were subjected to the compressive strength measurements and then the resulted crushed specimens were subjected to stopping of hydration process using solution of alcohol/acetone (1:1), followed by washing with acetone as recommended by [31, 32] in order to prevent further hydration

Mix no.	Water-cooled slag (WCS), %	Metakaolin (MK), %	Nano-kaolin (NK), %	NaOH, %	Sodium silicate, %	Sodium aluminate, %	Superplasticizer, %	Water/binder, %	T.M_2O/Al_2O_3	SiO_2/Al_2O_3	T.M_2O/SiO_2
Y0	40	60	0	15	5	-	1.50	0.22	1.063	2.04	0.31
Y1	40	59	1	15	5	-	1.50	0.22	1.048	2.01	0.31
Y3	40	57	3	15	5	-	1.70	0.22	1.060	2.03	0.31
Y5	40	55	5	15	5	-	1.90	0.24	1.060	2.03	0.31
Y7	40	53	7	15	5	-	2.12	0.24	1.056	2.02	0.31
Y9	40	51	9	15	5	-	2.30	0.24	1.054	2.01	0.31
X	40	60	0	15	5	5	1.50	0.24	1.163	1.88	0.36

Table 2. Composition of the geopolymer mixes (m%)
2. táblázat Alapanyagok kémiai összetétele (m%)

and for further analysis and followed by drying of the crushed specimens for 24 hrs at 80°C and then preserved in a well tight container until the time of testing.

2.4. Methods of investigation

Chemical analysis was carried out using Axios, WD-XRF Sequential Spectrometer (Panalytical, Netherland, 2009). Compressive strength tests were carried out using five tones German Brüf pressing machine with a loading rate of 100kg/min determined according to ASTM-C109 [33]. The XRD analysis was carried out using a Philips PW3050/60 Diffractometer. The data were identified according to the XRD software. The microstructure of the hardened alkali activated water cooled slag was studied using SEM Inspect S (FEI Company, Netherland) equipped with an energy dispersive X-ray analyzer (EDX). The removal of free water was accomplished by using alcohol/acetone method as recommended as recommended by [31, 32]. Transmission Electronic Microscopic (TEM) (type JEOL – JEM – 1230) of magnification up to 60000 was to measure the particle size of the nanoparticles. Bonding characteristics of the alkali activated specimens were analyzed using a Jasco-6100 Fourier transformed infrared spectrometer FTIR. Test sample was ground and uniformly mixed with KBr at a weight ratio KBr: specimen=200:1. The mixture, 0.20 g was pressed to a disk of 13 mm in diameter for analysis at 8 t/cm^2. The wave number was ranging from 400 to 4000 cm^{-1} [34, 35].

3. Results and discussion

3.1. Mineralogical investigation

Fig. 4, shows XRD pattern of 90 days alkali activated slag / MK (40: 60, wt.%) geopolymer mixes incorporated various NK content from 0 up to 9% as a partial replacement of MK. Pattern illustrate a band in the region of 6° to 10° 2θ for aluminosilicate gel and band in the region of 25° to 35° 2θ characterizing glassy phase of geopolymer constituents, the formation of intense peak of Faujasite of zeolite, zeolite A as well as sodalite in the control mix along with a sharp intense peaks for metastable phases of hydroxysodalite favours the lower geopolymer characteristic as known by their lower branching ability, the previous notice comes in accordance with Zuhua et al. [36], where the crystalline zeolite phases are destructive to the consistent distribution of geopolymers.

Addition of 1% NK results in decreasing crystalline zeolites as the nanomaterials offers a nucleation sites [29, 30] or geopolymer accumulation and so increases in the formed amorphous constituents in addition to shifting of the geopolymer region into lower 2θ, reflecting the increased amorphous constituents on the expense of the crystalline geopolymer. Increasing NK to 5% results in an extra enhancement in the geopolymerization reactions as the possibility for extra nucleation sites facilitate the accumulation and activation of the formed geopolymer as well as formation of CSH phases as allocated at 29.4° as well as Reversedite at 5.5 and 7.2°, where the formed CSH results from the interaction of freely dissolved silica with Ca species in the matrix forming CSH, in spite this binder can positively affect the structure by acting as nucleation sites for geopolymer formation and crystallization [37] as reflected on the mineralogical and structural composition of the formed geopolymer which can be in coherent with the increased Si/Al ratio (2.03) with NK forming poly-sialate siloxy chains, as well as T.M_2O/A_2O_3 which favours the amorphous geopolymer formation than crystalline one.

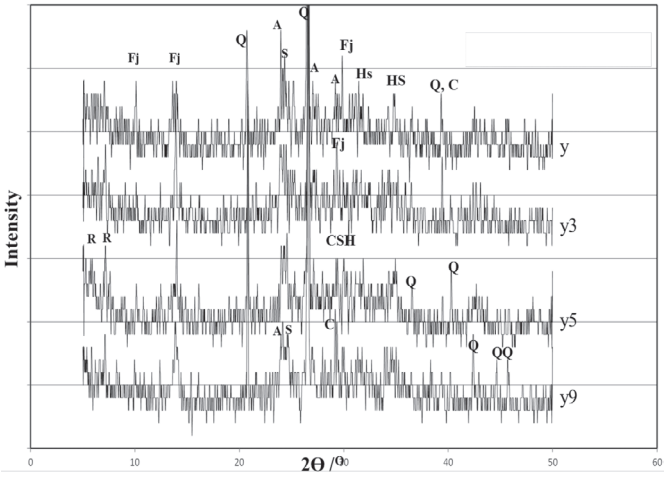

Fig. 4. XRD pattern of 90 days alkali activated MK-slag Geopolymer specimens having various NK rations as a partial replacement of metakaoline (Q: Quartz, A: ZeoliteA, FJ: Faujastine, R: Reversedite, CSH: Calcium silicate hydrate, S: Sodalite, HS: Hydroxysodalite, C: Calcite)

4. ábra 90 napos korú alkáli aktivált MK-kohósalak geopolimer keverékek röntgendiffraktogramjai különböző NK adagolás mellett [Q: kvarc, A: zeolit A, Fj: Faujasit, R: Reversedit, CSH: kalcium-szilikát-hidrát, S: szodalit, HS: hidroxoszodalit, C: kalcit]

However, further increase in NK content up to 9%, results again in an increase in the zeolitic phases as reflected on an increased broadness and intensity of Faujasite, sodalite and zeolite-A peaks, related mainly to the increased agglomeration of the added nanomaterial that will negatively affect the contact between the interacting geopolymer particles and so hinder the propagation of the geopolymerization reaction, so that the formed chains will be more prone to crystallization than propagation as well as formation of three dimensional network. Also, the agglomerated NK results in an increased porosity as well as increased carbonation within the matrix as indicated in calcite peak at 29.35°.

On investigating the effect of curing time up to 180 days on the control geopolymer specimen without NK, XRD pattern *Fig. 5*, illustrate the increase in CSH phases (reversedite, CSH) emphasizing an increased dissolution of binding slag's calcium and interacting with available free silica forming additional CASH binder phases in addition to CSH as a result of increased dissolution with time, also a noticeable increase in transformation of amorphous geopolymer structure into crystalline zeolite (Faujasite, sodalite, zeolite-A) with time is predominant which confirmed by the increased intensity of the previous phases with time up to 90 days, however further time increase results in the decrease in the broadness of the zeolite phases as a results of nucleation effect by CSH which facilitate and offer nucleation sites for geopolymer condensation and so hinder crystallization of geopolymer, then strengthen the formed matrix with time. There is small peak for calcite at 23.05° which may be resulted from the carbonation of CSH as well as any free alkalis within the matrix.

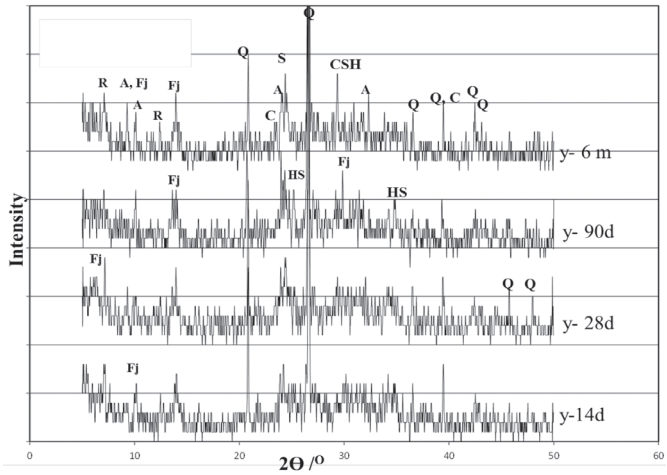

Fig. 5. XRD pattern of alkali activated control Geoplymer specimens MK-salg cured up to 180 days (Q: Quartz, A: ZeoliteA, FJ: Faujastine, R: Reversedite, CSH: Calcium silicate hydrate, S: Sodalite, HS: Hydroxysodalite, C: Calcite)

5. ábra 180 napos korú alkáli aktivált kontroll MK-kohósalak geopolimer keverékek röntgendiffraktogramjai [Q: kvarc, A: zeolit A, Fj: Faujasit, R: Reversedit, CSH: kalcium-szilikát-hidrát, S: szodalit, HS: hidroxoszodalit, C: kalcit]

Increasing in the activator by adding 5% sodium aluminate, results in an increase in the available sodium within the matrix which undergoes carbonation as depicted from increased calcite content in *Fig. 6*, also the increased sodium cations suppressed the propagation of geopolymer network and favours the oligomer formation as well as short chains geopolymer which will be susceptible to crystallization into zeolite as come in accordance with increased Faujasite and hydroxysodalite peaks [34] as compared with the control mix without aluminate source.

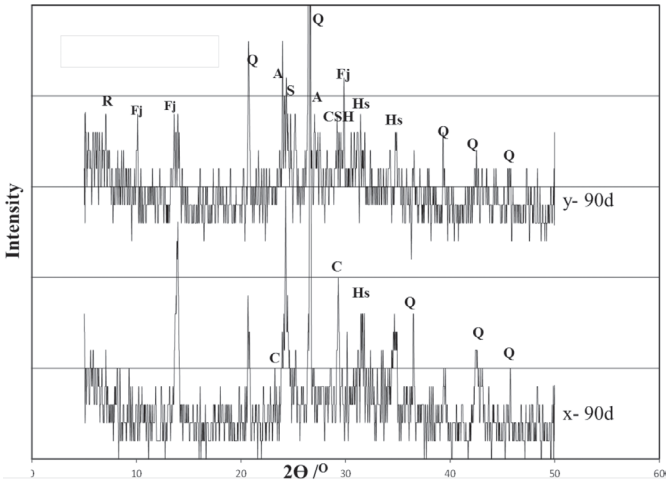

Fig. 6. XRD pattern of 90 days alkali activated slag/MK Geoploymer specimens activated by various activators (Q: Quartz, A: ZeoliteA, FJ: Faujastine, R: Reversedite, CSH: Calcium silicate hydrate, S: Sodalite, HS: Hydroxysodalite, C: Calcite)

6. ábra 90 napos korú alkáli aktivált MK-kohósalak geopolimer keverékek röntgendiffraktogramjai különböző aktivátorok alkalmazása esetén [Q: kvarc, A: zeolit A, Fj: Faujasit, R: Reversedit, CSH: kalcium-szilikát-hidrát, S: szodalit, HS: hidroxoszodalit, C: kalcit]

3.2. FTIR investigations

FTIR spectra of 90 days cured MK/slag geopolymer specimens having various NK content as a partial replacement of metakaolin are shown in *Fig. 7*. The characteristics bands for the present geopolymer structure are: hydration groups and combined water allocated for stretching vibration of O-H bond at about 3450 cm^{-1} and bending vibration for H-O-H at about 1640 cm^{-1}, stretching vibration of CO_2 located at about1430-1450 cm^{-1}, asymmetric stretching vibration (Si–O–Si) at about 1060 cm^{-1} for non-solubilized silica where T=Si or Al, asymmetric stretching vibration (Ti–O–Si) at about 975 cm^{-1} where T=Si or Al, out of plane bending vibration of CO_2 at about 870 cm^{-1}, symmetric stretching vibration (Si–O–Si)in the region 650-680 cm^{-1} and bending vibration (Si–O–Si and O–Si–O) in the region 420-440 cm^{-1}.

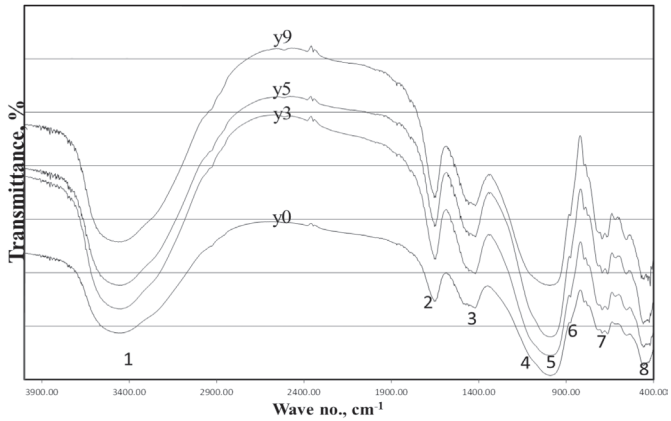

Fig. 7. FTIR spectra of 90 days cured (40 °C and 100% R.H.) MK-slag geopolymer specimens having various NK content [1: Stretching vibration of O-H bond; 2: Bending vibrations of (HOH); 3: Stretching vibration of CO_2; 4: Asymmetric stretching vibration (Si-O-Si); 5: Asymmetric stertching vibration (T-O-Si); 6: Symmetric stretching vibration of CO_2; 7: Symmetric stretching vibrations (Si-O-Si); 8: Bending vibration (Si-O-Si and O-Si-O)]

7. ábra 90 napos korú (40 °C, 100% RH) MK-kohósalak geopolimer keverékek FTIR spektrumai különböző NK adagolás mellett [1: Vegyértékrezgés O-H kötés, 2: Deformációs rezgés (HOH), 3: Vegyértékrezgés CO_2, 4: Aszimmetrikus vegyértékrezgés (Si-O-Si), 5: Aszimmetrikus vegyértékrezgés (T-O-Si), 6: Szimmetrikus vegyértékrezgés CO_2, 7: Szimmetrikus vegyértékrezgés (Si-O-Si), 8: Deformációs rezgés (Si-O-Si és O-Si-O)]

The pattern indicates an increased growth in the hydration bands and combined water at about 3400 and 1600 cm^{-1} with increasing NK increase up to 5% (Y5), then subjected to decrease with further NK increase up to 9%, this can be linked to the enhancement of NK [29, 30] in facilitating the interaction of free dissolved Ca and Si species forming nucleation sites for geopolymer accumulation [37] in addition to the their strengthen effect forming hydration materials (CSH, CASH) that acquire more water content in addition to the chemically combined water within the matrix structure.

It can be seen a gradual increase in the main asymmetric band for T-O-Si which related to the amorphous geopolymer structure with NK as a results of increasing the enhancement effect with NK addition up to 5% NK in addition to the shifting of the asymmetric band into lower wave number (958 cm^{-1}) as a results of increasing of the vitreous enhancement effect of NK by the formation of agglomerated bundles that segregate the reacting geopolymer chains which then underwent crystallization and inhibited the formation of more branched geopolymer structure with NK, however further increase of NK results in an increased broadness of the previous band and shifting a higher wave number with the presence of shoulder at about 1100 cm^{-1} for non-solublized silica, which linked directly to the negative effect of increased NK.

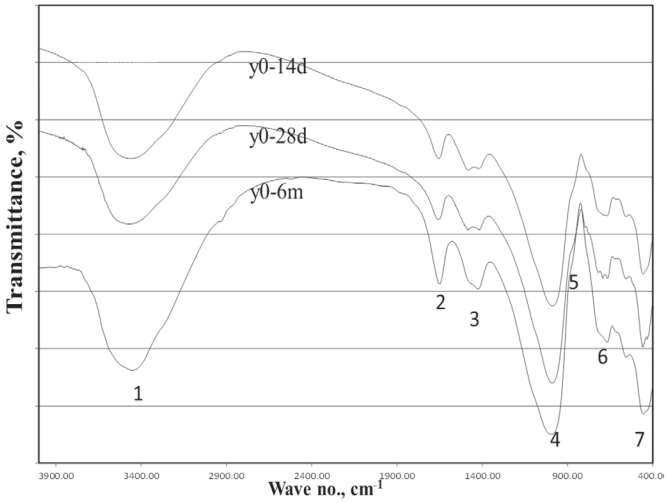

Fig. 8. FTIR spectra of control MK-geopolymer specimens cured up to 180 days [1: Stretching vibration of O-H bond; 2: Bending vibrations of (HOH); 3: Stretching vibration of CO_2; 4: Asymmetric stretching vibration (T-O-Si); 5: Symmetric stretching vibration of CO_2; 6: Symmetric stretching vibrations (Si-O-Si); 7: Bending vibration (Si-O-Si and O-Si-O)]

8. ábra 180 napos korú kontroll MK-kohósalak geopolimer keverékek FTIR spektrumai különböző NK adagolás mellett [1: Vegyértékrezgés O-H kötés, 2: Deformációs rezgés (HOH), 3: Vegyértékrezgés CO_2, 4: Aszimmetrikus vegyértékrezgés (T-O-Si), 5: Szimmetrikus vegyértékrezgés CO_2, 6: Szimmetrikus vegyértékrezgés (Si-O-Si), 7: Deformációs rezgés (Si-O-Si és O-Si-O)]

The appearance of bands in the regions of 1430-1450 cm^{-1} (ν C–O), and 867 cm^{-1} (δ C–O) are typical of $CO3^{2-}$ vibrational groups, present in inorganic carbonates [38], the increased contents of GBFS also lead to the growth of the carbonate band as discussed above, showing that the carbonates identified in this raw material do not react significantly under alkaline activation conditions [39]. These notices are in alignment with the XRD data where the amorphous vitreous structure increases up to 5% as well as increase in binding CSH phases that has an important role in binding the reacting materials however it may interfere with the required silica needed for geopolymer formation and accumulation [40].

Investigating the effect of increasing the curing time on the control geopolymer mix without NK (see *Fig. 8*), results in gradual increase in the main asymmetric band at about 950 cm^{-1} up to sharp increase at 6 months, as a results of increasing the rate of geopolymer formation and accumulation in the open pores resulting in the formation of well compacted structure, this is in consistent with the increased hydration band at about 3450 cm^{-1}, reflecting the increased combined water content in the geopolymer network as well as the formed CSH and CASH phases. It can be noticed also the splitting of the carbonation bands at about 1450 cm^{-1}, indicating the distorted nature of the formed carbonate as well as exposure of CSH binding phases into air carbonation [41, 42], this splitting turned to be diminished with time indicating the stability of the formed CSH against air carbonation.

3.3. SEM Observation

Microstructure of the control MK-slag geopolymer specimens without NK and cured at 90 and 180 days are shown in *Fig. 9*. It can be noticed that morphology of geopolymer specimens cured up to 90 days (*Fig. 9.a*), the coexistence of the aluminosilicate gel and the amorphous geopolymer in addition to CSH which fill mostly all the voids within the matrix, however increasing curing time to 180 days (*Fig. 9.b*) results in an increased transformation of the aluminosilicate gel into geopolymer plates that spread and forming a homogeneous structure; this is in coincide with the XRD and FTIR explanations.

Replacing MK by NK from 0 to 9% cured at 90 days *Fig. 10*, where the transformation of aluminosilicate gel in the control mix (*Fig. 10.a*) into geopolymer plates for mix containing 1% NK (*Fig. 10.b*) is a major feature as a result of the enhancement effect of NK in forming a nucleation sites for gel growth and precipitation. The previous nucleation illustration emphasized by increased formation of dense geopolymer plates that spread and fill most of the matrix forming a dense and well compact structure, where the added NK offers an extra nucleation sites for geopolymer growth in addition to the formed CSH by enhanced interaction of dissolved Ca and Si species (*Fig. 10.c*). On the other hand, further increase in NK to 9% results in the formation of agglomerates as a results of incomplete dispersion of high nano dose, these agglomerates results in the formation of weak zones and so result in formation of heterogeneous structure with many pores that spread within the structure,

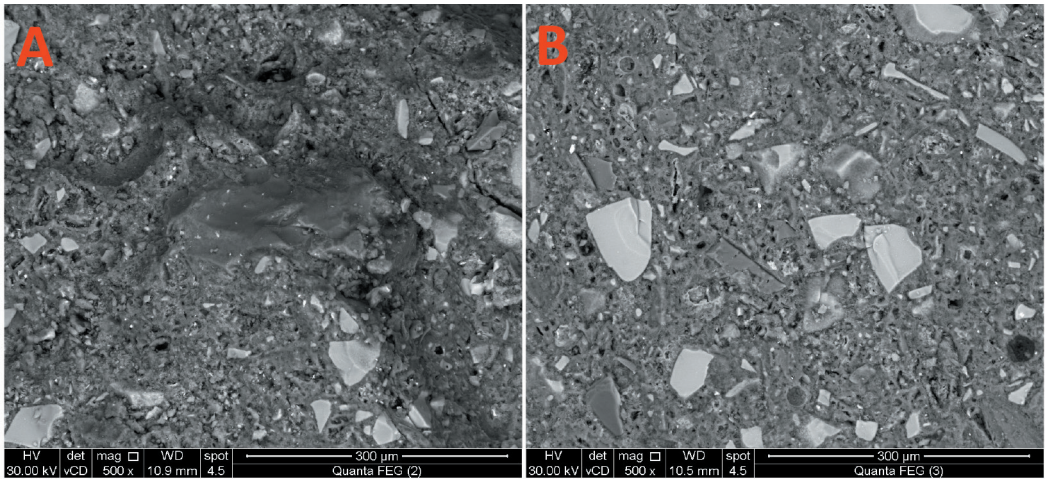

Fig. 9. SEM micrographs of alkali activated control Geopolymer specimens composed af 40% slag and 60% metakaoline cured at: A) 90 days B) 180 days

9. ábra Geopolimer keverékek (40% kohósalak, 60% metakaolin) elektronmikroszkópos felvételei különböző utókezelés mellett, a) 90 napig, b) 180 napig tartó utókezelés

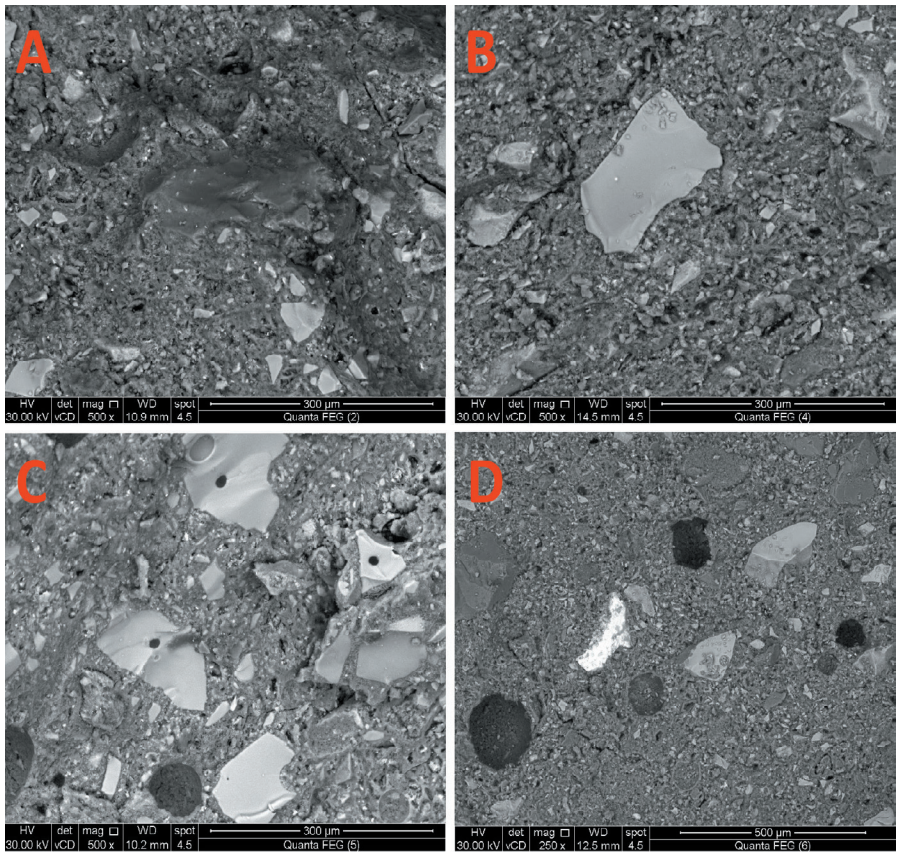

Fig. 10. SEM micrographs of 90 days alkali activated Geopolymer specimens having various Nanokaolin content. A) 0% NK, B) 3% NK, C) 5% NK, and D) 9% NK

10. ábra 90 napos korú alkáli aktivált geopolimer keverékek elektronmikroszkópos felvételei különböző nano-kaolin adagolás mellett, a) 0% NK, b) 3% NK, c) 5% NK, d) 9% NK

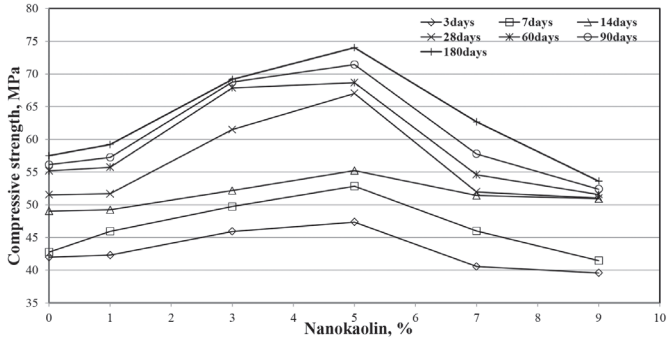

Fig. 11. Compressive strength of alkali activated MK-slag geopolymer specimens with various NK contents ratios as partial replacement of metakaoline cured up to 180 days

11. ábra Alkáli aktivált MK-kohósalak geopolimer keverékek nyomószilárdsága különböző NK adagolás és utókezelési időtartam mellett, 180 napos korig

these agglomerates inhibit the intact between geopolymer chains and so results in the formation less dense geopolymer structure (*Fig. 10.d*).

3.4. Compressive strength properties

The results of compressive strength for hardened MK/slag geopolymer mixes incorporated various NK content and cured in 100% relative humidity at 40°C up to 180 days are shown in *Fig. 11*. Results showed an increase of strength for all mixes along with hydration age as attributed to the continuing pozzolanic reaction as well as continuous growth of the geopolymer chains forming tightly bound structure, also the strength increase with NK up to 5%, and then subjected to gradual decrease with further NK addition. This increase with NK can be explained by increased geopolymer chain networks as results of increased nucleation sites for gel growth, in addition to the enhancement of NK to the interaction of dissolved Ca supplied by the GBFS with some of the excess dissolved silicate present, forming additional strengthen binding materials in addition to their role in providing nucleating agent for geopolymer formation and accumulation [43, 44], as illustrated clearly from XRD, FTIR, and SEM micrographs.

The decreased compressive strength up on increasing NK ratio more than 5% aroused primarily from incomplete dispersion of added nanomaterial forming agglomerates and result in formation of weak zones within the matrix providing more pores with susceptible for carbonation, as well as inhibiting the interaction and growth of the geopolymer networks. These previous findings confirmed with the XRD and FTIR which illustrated the growth of the amorphous geopolymer as well as CSH with NK up to 5%, while suffering of amorphous constituents as well as shifting of the main asymmetric geopolymer band to higher wave number favouring the zeolite formation than amorphous geopolymer increase, emphasizing the segregation effect of NK and so zeolite structure with lower chains formed on the expense of three dimensional networks, also the increased carbonate with NK increase (9%) confirms the presence of more pores as well as the presence of available cations exposed for carbonations. This increased porosity coincide with SEM micrographs illustrations where an increased pores in high NK content is the predominant feature.

However, on comparing mechanical compressive strength of control geopolymer mix specimens activated by sodium hydroxide, silicate and aluminate and cured up to 180 days (*Fig. 12*), where adding aluminate source in spite benefits the geopolymerization by adding extra sodium cations and alumina source, it lowered the SiO_2/Al_2O_3 (1.88 as compared with 2.04 for non-aluminate activator source) and so transferred from the category of polysialate-siloxo into polysilate species which known by its lowering branching ability than the previous one, in addition exceeding of the sodium cation over the required balancing ions necessary for charge balancing as resulted from Table 2 which gives the values of 1.163 and 0.36 for $T.M_2O/Al_2O_3$ and $T.M_2O/SiO_2$ and resulting in:

1. Sodium cations, which are normally presented at high concentrations in the geopolymeric systems, are specifically adsorbed ions on the surface of geopolymer particles changing

the surface speciation according to the following chemical Equation:

> T–OH + Na^+ <=> T–ONa + H^+

The stability area of >T–O-Na surface species is pH dependent and is located at extremely high pH values [45].

2. The sodium cations adsorption in highly alkaline conditions consumes the surface species (>T–OH and >T–O–), on which the chemical bonding between the insoluble solid particles and the geopolymeric framework takes place in the final stage of the geopolymerization process. Thus, the resulted geopolymeric materials have low mechanical strength [34].

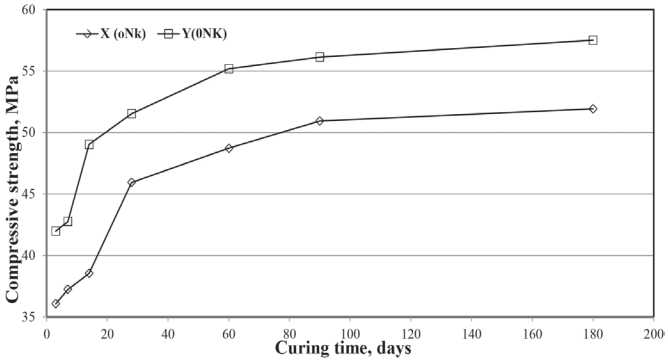

Fig. 12. Compressive strength of alkali activated MK-slag geopolymer specimens activated by different activators cured up to 180 days

12. ábra Alkáli aktivált MK-kohósalak geopolimer keverékek nyomószilárdsága különböző aktivátor és utókezelési időtartam mellett, 180 napos korig

The compressive strength confirmed and emphasized by XRD and FTIR where an increased amorphous geopolymer structure in the control mix without aluminate source as compared with one aluminate activator mix, where an increased Faujasite content in XRD as well as shifting to higher wave number in FTIR as a results of increased zeolite. The compressive strength results give a values of 45.93, 50.93 and 51.90 MPa after 28, 60 and 90 days, respectively, for aluminate activated mix, while gives 51.53, 56.13 and 57.51 MPa for non-aluminate mix geopolymer specimen which can be applied in various building application purposes.

4. Conclusions

The most important findings of the present paper are summarized below:

1. Addition of NK results in better enhancement in mechanical and morphological by using NK up to 5%, however further increase results in an agglomeration and decrease in efficiency of added nanomaterials.
2. SEM micrographs have proved an increased enhancement in microstructural properties of the NK-mixes up to formation of dense and homogenous morphological shape when using 5% NK, whilst an increase in the matrix porosity is a common feature of higher NK-mixes.
3. XRD and FTIR spectra confirm an intense amorphous geopolymer structure up on using 5% NK, while an increased crystalline phase with an increased carbonate bearing compounds are predominant with further NK.
4. Geopolymer mixes possess high mechanical properties that exceed 50 MPa after 28 days for control mix and increased with further NK up to 5%, giving a value of 67 MPa at 28 days and 71 MPa at 6 months, which can be used in various building applications as infrastructure as well as fire resistant building materials.
5. Using sodium aluminate activating source results in lowering in mechanical and physical characteristics of the produced specimens whilst their strength values reaches 45 MPa and 52 MPa after 28 and 90 days of curing.

Conflict of Interest: The authors declare that they have no conflict of interest.

References

[1] Taylor, H.F.W. (1964): The Chemistry of Cements, Vol. 1, 1st Ed., Academic Press, London.

[2] Gani, M.S.J. (1997): Cement and Concrete, 1st Ed., Chapman and Hall, London.

[3] Richardson, I.G. – Cabrera, J.G. (2000): The nature of C–S–H in model slag cements, *Cement and Concrete Composites*, Vol. 22, No. 4, pp. 259-266. https://doi.org/10.1016/S0958-9465(00)00022-6

[4] Van Jaarsveld, J.G.S. – van Deventer, J.S.J. – Lorenzen, L. (1997): The potential use of geopolymeric materials to immobilise toxic metals: Part I. *Theory and applications, Minerals Engineering*, Vol. 10, No. 7, pp. 659-669. https://doi.org/10.1016/S0892-6875(97)00046-0

[5] Van Jaarsveld, J.G.S. – van Deventer, J.S.J. (1999): The effect of metal contaminants on the formation and properties of waste-based geopolymers, *Cement and Concrete Research*, Vol. 29, No. 8, pp. 1189-1200. https://doi.org/10.1016/S0008-8846(99)00032-0

[6] Xu, H. – van Deventer, J.S.J. (2000): The geopolymerization of alumino-silicate minerals, *International Journal of Mineral Processing*, Vol. 59, No. 3, pp. 247-266. https://doi.org/10.1016/S0301-7516(99)00074-5

[7] Phair, J.W. – van Deventer, J.S.J. (2002): Characterization of fly-ash based geopolymeric binders activated with sodium aluminate, *Industrial and Engineering Chemistry Research*, Vol. 41, pp. 4242– 4251. https://doi.org/10.1021/ie010937o

[8] Alonso, S. – Palomo, A. (2001): Alkaline activation of metakaolin and calcium hydroxide mixtures: influence of temperature, activator concentration and solids ratio, *Materials Letters*, Vol. 47, No. 1–2, pp. 55-62. https://doi.org/10.1016/S0167-577X(00)00212-3

[9] Alonso, S. – Palomo, A. (2001): Calorimetric study of alkaline activation of calcium hydroxide–metakaolin solid mixtures, *Cement and Concrete Research*, Vol. 31, No. 1, pp. 25-30. https://doi.org/10.1016/S0008-8846(00)00435-X

[10] Frias, M. – Cabrera, J. (2001): Influence of MK on the reaction kinetics in MK/lime and MK-blended cement systems at 20°C, *Cement and Concrete Research*, Vol. 31, No. 4, pp. 519-527. https://doi.org/10.1016/S0008-8846(00)00465-8

[11] Frias, M. – Sanchez de Rojas, M.I. – Cabrera, J. (2000): The effect that the pozzolanic reaction of metakaolin has on the heat evolution in metakaolin-cement mortars, *Cement and Concrete Research*, Vol. 30, No. 2, pp. 209-216. https://doi.org/10.1016/S0008-8846(99)00231-8

[12] Cabrera, J. – Rojas, M.F. (2001): Mechanism of hydration of the metakaolin–lime–water system, *Cement and Concrete Research*, Vol. 31, No. 2, pp. 177-182. https://doi.org/10.1016/S0008-8846(00)00456-7

[13] Coleman, N.J. – McWhinnie, W.R. (2000): The solid state chemistry of metakaolin-blended ordinary Portland cement, *Journal of Materials Science*, Vol. 35, No. 11, pp. 2701–2710. https://doi.org/10.1023/A:1004753926277

[14] Aiu, M.(2006): The Chemistry and Physics of Nano-Cement, *Loyola Mary Mount University*, Advisor: Dr. C.P. Huang Submitted to: NSF-REU University of Delaware August 11, 2006.

[15] Li, H. – Xiao, H. – Ou., Jinping (2004): Microstructure of cement mortar with nano particles, *Composites Part B: Engineering*, Vol. 35, No. 2, pp. 185-189. https://doi.org/10.1016/S1359-8368(03)00052-0

[16] Ginebra, M.P. – Driessens, F.C.M. – Planell, J.A. (2004): Effect of the particle size on the micro and nano structural features calcium phosphate cement: a kinetic analysis, *Biomaterials*, Vol. 25, No. 17, pp. 3453-3462. https://doi.org/10.1016/j.biomaterials.2003.10.049

[17] Zins, D. – Cabuil, V. – Massart, R. (1999): New aqueous magnetic fluids, *Journal of Molecular Liquids*, Vol. 83, No. 1–3, pp. 217-232. https://doi.org/10.1016/S0167-7322(99)00087-2

[18] Ge, Z. – Gao, Z. (2008): Applications of Nanotechnology and Nano materials in Construction, *First International Conference on Construction In Developing Countries (ICCIDC-I)* "Advancing and Integrating Construction Education, Research & Practice" August 4-5, 2008, Karachi, Pakistan

[19] Hanehara, S. – Ichikawa., M. (2001): Nanotechnology of cement and concrete, *Journal of the Taiheiyo Cement Corporation*, Vol. 141, pp. 47-58.

[20] Scrivener, K. L. (2009): Nanotechnology and cementitious materials. In: Bittnar Z, Bartos PJM, Nemecek J, Smilauer V and Zeman J, editors. *Nanotechnology in construction: proceedings of the NICOM3* (3rd international symposium on nanotechnology in construction). Prague, Czech Republic. pp. 37–42.

[21] Abo-El-Enein, S.A. – Amin, M.S. – El-Hosiny, F.I. – Hanafi, S. – ElSokkary, T.M. – Hazem, M.M. (2014): Pozzolanic and hydraulic activity of nano-metakaolin, *HBRC Journal*, Vol. 10, No. 1, pp. 64-72. https://doi.org/10.1016/j.hbrcj.2013.09.006

[22] Morsy, M.S., Alsayed, S.H., Aqel, M. (2011) Hybrid effect of carbon nanotube and nano-clay on physico-mechanical properties of cement mortar, *Construction and Building Materials*, Vol. 25, No. 1, pp. 145-149. https://doi.org/10.1016/j.conbuildmat.2010.06.046

[23] Morsy, M.S. – Al-Salloum, Y.A. – Almusallam, T. – Abbas, H. (2014): Effect of nano-metakaolin addition on the hydration characteristics of fly ash blended cement mortar, *Journal of Thermal Analysis and Calorimetry*, Vol. 116, No. 2, pp. 845–852. https://doi.org/10.1007/s10973-013-3512-6

[24] Morsy, M.S. – Al-Salloum, Y.A. – Abbas, H. – Alsayed, S.H. (2012): Behavior of blended cement mortars containing nano- metakaolin at elevated temperatures, *Construction and Building Materials*, Vol. 35, pp. 900–905. https://doi.org/10.1016/j.conbuildmat.2012.04.099

[25] Baueregger m, S. – Lei, L. – Plank, J. – Perello, M. (2015): Use of Nano-MK for early strength enhancement of Portland cement, *Nano-technology in construction: Proceeding of NICOM5*, 199 Springer international publishing, 199-206, Switzerland, 2015.

[26] Khater, H.M. – El-Sabbagh, B.A. – Fanny, M. – Ezzat, M. – Lottfy, M. (2013): Effect of Nano-Clay on Alkali Activated Water-Cooled Slag Geopolymer, *British Journal of Applied Science and Technology*, Vol. 3, No. 4, pp. 764-776. https://doi.org/10.9734/BJAST/2013/2690

[27] Kakali, G. – Perraki, T. – Tsivilis, S. – Badogiannis, E. (2001): Thermal treatment of kaolin: the effect of mineralogy on the pozzolanic activity, *Applied Clay Science*, Vol. 20, No. 1-2, pp. 73–80. https://doi.org/10.1016/S0169-1317(01)00040-0

[28] Wenying, G. – Guolin, W. – Jianda, W. – Ziyun, W. – Suhong, Y. (2008): Preparation and Performance of Geopolymers, *Journal of Wuhan University of Technology – Materials Science Edition*, Vol. 23, No. 3, pp. 326–330. https://doi.org/10.1007/s11595-007-3326-0

[29] Khater, H.M. (2012): Effect of Calcium on Geopolymerization of Aluminosilicate Wastes, *Journal of Materials in Civil Engineering*, Vol. 24, No. 1, https://doi.org/10.1061/(ASCE)MT.1943-5533.0000352

[30] Khater, H.M. (2013): Effect of Silica Fume on the Characterization of the Geopolymer Materials, *International Journal of Advanced Structural Engineering*, Vol. 5, No. 12, https://doi.org/10.1186/2008-6695-5-12

[31] Khater, H.M. (2013): Effect of cement Kiln dust on geopolymer composition and its resistance to sulfate attack, *Green materials Journal,* Vol. 1, No. 1, pp. 36-46. https://doi.org/10.1680/gmat.12.00003

[32] El-Sayed, H.A. – Abo El-Enein, S.A. – Khater, H.M. – Hasanein, S.A. (2011): Resistance of Alkali Activated Water Cooled Slag Geopolymer to Sulfate Attack, *Ceramics – Silikáty*, Vol. 55, No. 2, pp. 153-160.

[33] ASTM C109M (2016) Standard Test Method for Compressive Strength of Hydraulic Cement Mortars.

[34] Panias, D. – Giannopolou, L.P. – Peraki, T. (2007): Effect of synthesis parameters on the mechanical properties of fly ash-based geopolymers, *Colloids and Surfaces A: Physicochemical and Engineering Aspects*, Vol. 301, No. 1–3, pp. 246-254. https://doi.org/10.1016/j.colsurfa.2006.12.064

[35] Bakarev, T. (2006): Thermal behavior of geopolymer prepared using class F fly ash and elected temperature curing, *Cement and Concrete Research*, Vol. 36, No. 6, pp. 1134-1147. https://doi.org/10.1016/j.cemconres.2006.03.022

[36] Zuhua Z. – Xiao, Y. – Huajun, Z. – Yue, C. (2009): Role of water in the synthesis of calcined kaolin-based geopolymer, *Applied Clay Science*, Vol. 43, No. 2, pp. 218-223. https://doi.org/10.1016/j.clay.2008.09.003

[37] Temuujin, J. – Van Riessen, A. – Williams, R. (2009): Influence of calcium compounds on the mechanical properties of fly ash geopolymer pastes, *Journal of Hazardous Materials*, Vol. 167, No. 1–3, 15 pp. 82-88. https://doi.org/10.1016/j.jhazmat.2008.12.121

[38] Garcia-Lodeiro, I. – Fernandez-Jimenez, A. – Palomo, A. – Macphee, D.E. (2010): Effect on fresh CS-H gels of the simultaneous addition of alkali and aluminium, *Cement and Concrete Research*, Vol. 40, No. 1, pp. 27-32. https://doi.org/10.1016/j.cemconres.2009.08.004

[39] Bernal, S.A. – Rodríguez, E.D. – Mejia de Gutiérrez, R. – Provis, J-L. – Delvasto, S. (2012): Activation of Metakaolin/Slag Blends Using Alkaline Solutions Based on Chemically Modified Silica Fume and Rice Husk Ash, *Waste and Biomass Valorization*, Vol. 3, No. 1, pp. 99–108. https://doi.org/10.1007/s12649-011-9093-3

[40] Catalfamo, P. – Di Pasquale, S. – Corigliano, F. – Mavilia, L. (1997): Influence of the calcium content on the coal fly ash features in some innovative applications, *Resources, Conservation and Recycling*, Vol. 20, No. 2, pp. 119-125. https://doi.org/10.1016/S0921-3449(97)00013-X

[41] Kalinkin, A. M. – Politov, A. A. – Boldyrev, V. V. – Kalinkina, E. V. – Makarov, V. N. – Kalinnikov V. T. (2002): Study of Mechanical Activation of Diopside in a CO_2 Atmosphere. *Journal of Materials Synthesis and Processing*, Vol. 10, No. 1, pp. 61–67. https://doi.org/10.1023/A:1021057231463

[42] Kalinkin, A. M. – Kalinkina, E. V. – Politov, A. A. – Makarov, V. N. – Boldyrev, V. V. (2004): Mechanochemical interaction of Ca silicate and aluminosilicate minerals with carbon dioxide. *Journal of Materials Science*, Vol. 39, No. 16–17, pp. 5393–5398. https://doi.org/10.1023/B:JMSC.0000039252.13062.63

[43] Van Deventer, J.S.J. – Provis, J.L. – Duxson, P. – Luckey, G.C. (2007): Reaction mechanisms in the geopolymeric conversion of inorganic waste to useful products, *Journal of Hazardous Materials*, Vol. 139, No. 3, pp. 506-513. https://doi.org/10.1016/j.jhazmat.2006.02.044

[44] Lee, W.K.W. – Van Deventer, J.S.J. (2002): The effect of ionic contaminants on the early age properties of alkali-activated fly ash based cements, *Cement and Concrete Research*, Vol. 32, No. 4, pp. 577-584. https://doi.org/10.1016/S0008-8846(01)00724-4

[45] Skoufadis, C. – Panias, D. – Paspaliaris, I. (2003): Theoretical determination of electrochemical properties of boehmite–water interface, as a tool for understanding the mechanism of boehmite precipitation, in: *European Metallurgical Conference*, vol. 1, Hanover, Germany, 2003; pp. 321–338.

Ref.:
Khater, H. M. – **Abd el Gawwad,** H.: *Synthesis and characterization of MK/ Slag geopolymer composites enhanced by various ratios of nano kaolin*
Építőanyag – Journal of Silicate Based and Composite Materials, Vol. 69, No. 2 (2017), 40–48. p.
https://doi.org/10.14382/epitoanyag-jsbcm.2017.8

Nano-kaolin tartalmú MK/kohósalak geopolimerek szintézise és tulajdonságai

A cikk nano-kaolin tartalmú metakaolin/kohósalak geopolimer keverékek alkáli aktiválási lehetőségét mutatja be és ismerteti a C-A-S-H és N-A-S-H gél képződés részleteit. Aktivátorként 10% NaOH oldatot és 5% nátrium-szilikát oldatot használtak és a nano-kaolin adagolás 0 és 9% között változott. A kialakuló geopolimerek mechanikai tulajdonságait (nyomószilárdság) prizmatikus próbatesteken vizsgálták. A struktúra és fázisösszetétel vizsgálata során pásztázó elektronmikroszkópot, röntgendiffraktométert és infravörös spektroszkópot használtak. Az eredmények rávilágítottak, hogy a nano-kaolin adagolása 5%-os mennyiségig javítja a mikrostruktúrát és szilárdságnövekedést eredményez, de ennél nagyobb mennyiség adagolása agglomerációhoz és szilárdságcsökkenéshez vezet. Nátrium-aluminát aktivátor adagolása szilárdságcsökkenést eredményez a zeolit képződés következtében.

Kulcsszavak: Nano-kaolin, Geopolimer, aktiválás, környezetbarát.